



Water masses in the Atlantic Ocean: water mass ages and ventilation

Mian Liu^{1,2} and Toste Tanhua²

¹School of Environmental Science and Engineering, Xiamen University of Technology, Xiamen, 361021, China

²GEOMAR Helmholtz Centre for Ocean Research Kiel, Marine Biogeochemistry, Chemical Oceanography, Wischhofstraße 5 1-3, 24148 Kiel, Germany

Correspondence to: Mian Liu (2023000069@xmut.edu.cn)

Abstract: The distribution of water masses, and the ventilation rates of these, are of significance to the thermohaline circulation and biogeochemistry of the world oceans. The distribution of the main water masses in the Atlantic Ocean is published in a companion study (Liu and Tanhua, 2021), their ages and ventilation time-scales are reported here by using observations of the

10 transient tracers, CFC-12 and SF₆. Two different definitions of water mass ages are presented; the mean-age representing an average age of a water mass, and the mode-age that better represents the advective time-scale. In general, ages increase with pressure and along the pathway of a water mass. The central waters in the upper layer obtain the mean-ages of up to ~100 years and the mode-ages of up to ~30 years. In the intermediate layer, the Antarctic Intermediate Water (AAIW) and the Mediterranean Water (MW) show gradients of water mass ages in the meridional and zonal direction respectively. The AAIW 15 obtains the highest mean-age of ~300 years and mode-age of ~80 years at 30 °N, while the MW shows the highest mean-age of ~400 years and mode-age of ~100 years in the equator region. As the dominant water mass in the deep and overflow layer, the North Atlantic Deep Water (NADW) from high northern latitudes obtains the highest mean-age of ~600 years and mode-age of ~100 years in the Antarctic Circumpolar Current (ACC) region at 50 °S. In the bottom layer, the Antarctic Bottom Water (AABW) from the Weddell Sea obtains the highest mean-age of ~600 years and mode-age of ~100 years in the equator. 20 As the continuation of AABW, the Northeast Atlantic Bottom Water (NEABW) obtains the highest mean-age of ~800 years and mode-age of ~120 years at 50 °N. The mode-age increases with the transport distance from formation area, accompanied by significant differences between the eastern and western basins. The mode-age is used to calculate the oxygen utilization rate (OUR) with apparent oxygen utilization (AOU) during the active transport in water masses. The western basin exhibits lower mode-age with higher oxygen (low AOU) due to the better ventilation. The OUR shows similar distribution to dissolved 25 oxygen (DO), indicating higher oxidation rate in the high oxygen region.

Key words: Water Mass, Atlantic Ocean, Transient Tracer, Mean- and Mode-age, Ventilation, GLODAPv2 data product



1 Introduction

The Atlantic Ocean is composed by several water masses distributed in distinct vertical layers along different density boundaries. Liu and Tanhua, (2021) defined the characteristics of 16 water masses that have been widely considered and studied due to their impacts on the ocean circulation and climate (e.g. Hall and Bryden, 1982; Bryden et al., 2005; Kuhlbrodt et al., 2007; Clark et al., 2012). Ventilation is a process that brings surface water to the ocean interior and thus transports surface anomalies from the upper layer. For obvious mass-conservation reasons, ventilation also bring deep water to the surface. This is a significant process for heat budgets and maintains the thermodynamic balance in the ocean (Talley, 2013; 30 Armour et al. 2016; Talley et al., 2016). In addition, the ventilation is also a key factor in the marine biogeochemistry that, for instance, transports oxygen and carbon dioxide into the abyssal layers (Tanhua et al., 2006; Ziska et al., 2013; Skinner et al., 35 2017). This process is thus a determinant for the oxygen concentration and carbon storage in the abyssal ocean interior (van Heuven et al., 2011; Ito et al., 2016; Schmidtko et al., 2017).

Early studies of the water mass ventilation are proposed by Sandström already in the early 20th century (Sandström, 1908; 40 1916). Sverdrup and Bjerknes also reported the impacts of ventilation and currents on the climate through the air-sea interactions (Sverdrup, 1940; Bjerknes, 1964). Hereafter many studies have been focusing on the ventilation. For instance, Dickson et al., (1994) estimated the formation and pathway of the North Atlantic Deep Water (NADW) based on the hydrodynamics, Orsi et al., (1999) investigated the circulation of the Antarctic Bottom Water (AABW) by using Chlorofluorocarbons (CFCs). Recent studies suggest that the intensity of ocean ventilation varies with environmental factors, 45 such as intensity of the westerly winds (e.g. Rahmstorf, 2010; Purkey et al., 2010; Morrison et al., 2015). Several studies investigate the regional scale or specific water masses, for instance, the upwelling of Circumpolar Deep Water (CDW) in the Southern Ocean (Tamsitt et al., 2017), or the ventilation in the South China Sea (Wang et al., 2021). However, few studies look at the ventilation over ocean basin scales, which is helpful to understand the effect of ocean-climate interactions, and in addition can provide a basis for the biogeochemical studies.

50 The water mass age is an important parameter to evaluate the ventilation and refers to as the elapsed time on the pathway. The CFCs and Sulfur hexafluoride (SF_6) are recognized as effective transient tracers for water masses and to estimate their ages (Fine, 2011). The concentrations of CFCs in surface seawater increased continuously following the increase of the atmospheric concentration since their introduction in the early 20th century (Gammon et al., 1982; Warner and Weiss, 1985). The use of CFCs as a tracer in the oceanography is well established (e.g. Bullister and Weiss, 1983; Doney and Bullister, 1992; Fine, 55 2010; 2011), and transient tracers is a core variable in the GO-SHIP repeat hydrography program. Similarly, the transient tracer is an Essential Ocean Variable (EOV) in the Global Ocean Observing System (GOOS) framework. SF_6 has been used as a new tracer since mid-1990s complementing the CFCs due to the reduction of CFCs in the atmosphere (Maiss et al., 1996; Bullister et al., 2002). The application of SF_6 is generally appropriate for recently formed water masses in the upper ocean (Tanhua et al., 2008), i.e. for well ventilated, or young, waters. The CFCs are used to trace the “old/deep” water masses (before mid-1990s 60 or partial pressure of CFC-12 lower than about 450 part per trillion, ppt), while the SF_6 is the better choice for recently formed shallow water masses (after mid-1990s or partial pressure of CFC-12 higher than about 450 ppt, Tanhua et al., 2008). In addition, the application of transient tracers also provides support to the hydrographic and biogeochemical field in calculating the upwelling velocity (Tanhua and Liu, 2015) or estimating the ventilation and anthropogenic carbon cycle (van Heuven et al., 2011; Tanhua et al., 2013; Patara et al., 2021).



65 The apparent oxygen utilization (AOU, $\mu\text{mol kg}^{-1}$) is an important indicator in characterizing the respiration of organic matter
consuming oxygen, and balancing the oxygen supply through ventilation and photosynthesis. The oxygen utilization rate (OUR,
 $\mu\text{mol kg}^{-1} \text{ yr}^{-1}$), which can be calculated from AOU and water mass age, is a significant parameter in estimating the
biogeochemical processes such as primary productivity or remineralization (e.g. Jenkins, 1982; Bender, 1990). The OUR has
been recognized to be a function of pressure for a long time (e.g. Tseitlin, 1992). However, recent studies suggest that the OUR
70 is the integrated oxygen consumption rate along the pathway of a water mass and represents a regional view of export flux
(Stanley et al., 2012; Koeve and Kähler, 2016). In this study, the OUR is calculated from water mass ages estimated from the
CFC-12 and SF₆. The change of OUR over time in different water masses are presented and the impacts from the currents and
topography are discussed.

75 In the study by Liu and Tanhua, (2021), the characteristics of main water masses in the Atlantic Ocean are defined by six key
properties, using the Global Ocean Data Analysis Project version 2 (GLODAPv2) data product as a source of unbiased data.
The static distribution of the water masses is estimated with the Optimal Multi-Parameter analysis (OMP analysis, Karstensen
and Tomczak, 1997; 1998). As a continuation of that work, here we estimate the ventilation of water masses in the Atlantic
Ocean with observations of transient tracers (CFC-12 and SF₆). The water mass ages are estimated and the OURs are calculated.
80 The goal of this study is to further improve the report of water masses in the Atlantic Ocean by adding the age as a measure of
ventilation, and to provide a hydrographic assistant for the biogeochemical researches.

2 Data and methods

2.1 Transient tracers and Inverse Gaussian Transit Time Distribution (IG-TTD)

Attempts have been made to find chemically stable with large dynamic ranges in seawater as tracers that can be reasonable
easily measured. The prerequisite for transient tracers is 1) the concentration in the atmosphere increases (or decreases)
85 monotonously in the history; 2) their surface concentration is equilibrium to the atmosphere, or the saturation state over time
can be estimated; 3) their input functions are known; 4) there are no sources or sinks in the ocean interior. The solubility (F)
of transient tracers in the seawater is a function of potential temperature (θ) and practice salinity (S) (Warner and Weiss, 1985;
Bullister et al., 2002).

90 By considering the diffusive ocean where mixing is important, Waugh et al., (2003) applied the concept of transit time
distribution (TTD, Hall and Plumb, 1994) to the ocean interior:

Tracer-age ($c(t)$) is the time that water mass takes from surface to the deeper layer.

$$c(t) = c_0(t - \tau);$$

Mean-age (Γ) shows the average of ages in different parts of a water sample from different pathways.

$$\Gamma = \int_0^\infty \xi G(\xi) d\xi;$$

95 Width (Δ^2) describes the mixing and the diffusion in the ocean.

$$\Delta^2 = \frac{1}{2} \int_0^\infty (\xi - \Gamma)^2 G(\xi) d\xi;$$



The relationship between all the above parameters is often assumed to follow the inverse Gaussian function.

$$G(t) = \sqrt{\frac{r^3}{4\pi\Delta^2 t^3}} \exp\left(-\frac{\Gamma(t-\Gamma)^2}{4\Delta^2 t}\right);$$

In this equation t , Γ and Δ describe the tracer-age, mean-age and the width of TTD. In the ocean reality, the mixing ratio (Δ/Γ) indicates the situation of advective (low ratio) or diffusive (high ratio). Although it is possible and conceivable that other solutions to the TTD than an Inverse Gaussian (IG) function best describes the ventilation age of a water mass, we apply the IG solution to the TTD in this work. For instance, Stöven and Tanhua, (2014) concludes that a 2-IG distribution is necessary to explain ventilation ages in the Mediterranean Sea. The TTD concept also assumes a steady state ocean, circulation, a condition that is often not fulfilled. For this application however we use the 1-IG concept since solving other possibilities is not possible with the few collocated transient tracer observations available. Based on the TTD determined from the tracer observations, Wang et al., (2021) estimated the OUR in the northern South China Sea.

2.2 Definitions in the age of a water mass: tracer-age, mean-age and mode-age

The concept of a water mass age is defined as the time elapsed from that a water mass was in contact with the atmosphere at the surface in the formation area (Thiele and Sarmiento, 1990). The concentrations of transient tracers (CFC-12 and SF₆ in units of mol kg⁻¹) can be observed directly in the interior ocean and the partial pressures can be calculated combining with the potential temperature (θ in °C) and practical salinity (S). With the TTD concept, three different flavors of water mass ages are often used as derived from observations of transient tracers; the tracer-age, the mean-age and the mode-age.

The tracer-age shows the elapsed time from the surface of the formation area to the interior ocean at the sampling location (Fig. 1, a) by simply matching the observed tracer fields with the atmospheric history of the tracers. In other words, the tracer-age assumes the ocean is purely advective, without diffusion. This definition is simple to apply as a TTD do not need to be considered, i.e. the TTD is only one spike. However, the diffusion cannot be neglected in the realistic oceans, so the actual ages of water masses are underestimated by the tracer-age. The concept of TTD is applied in order to correct such underestimation. A definition of mixing ratio (Δ/Γ , see below) is defined as the width of an Inverse Gaussian (IG) distribution over the ages to indicate the advective (low ratio) or diffusive (high ratio) situation. From the IG distribution, the mean-age and mode-ages can be calculated. The mean-age is obtained by the average value of all the different aliquots in one water sample by considering the transport time of different pathways (Fig. 1, b). This concept of water mass age is often useful for biogeochemical studies. In other cases, such as when discussing the transport times of water masses from the formation area, the mode-age concept is useful. From the physical perspective, the mode-age reflects the age of the dominate water mass in the sample, i.e. the mode-age shows the time (t) when the Inverse Gaussian Distribution (G(t)) reaches the maximum (Fig. 1, b).

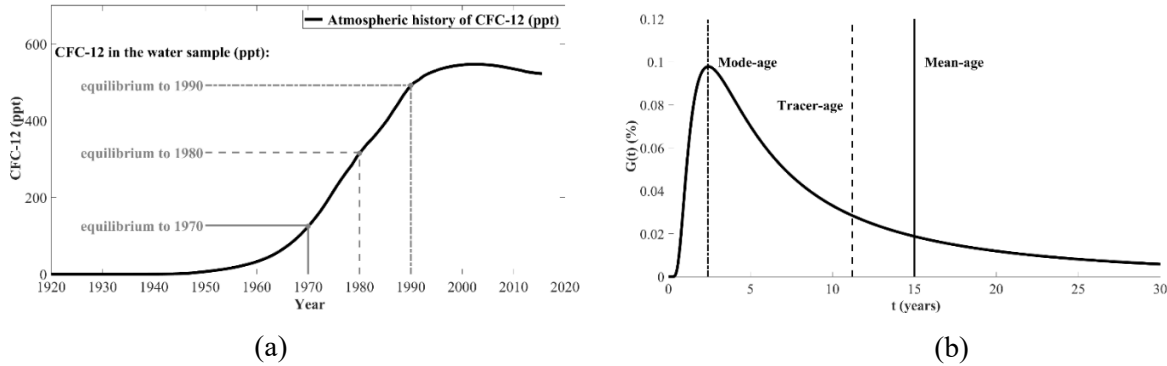


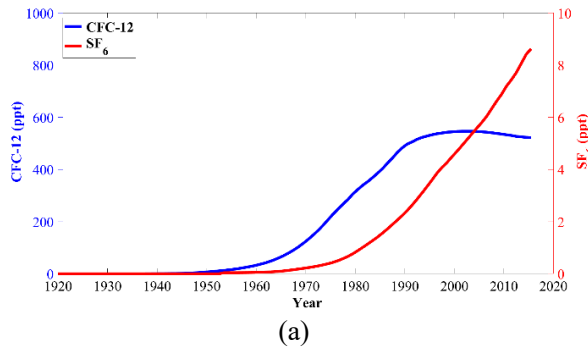
Figure 1. Concepts of three flavors of water mass ages.

(a) The tracer-age shows the transient tracers in the water samples are equilibrium to which year of the atmospheric history and assumes the ocean as purely advective; (b) The concept of tracer-age, mean-age and mode-age are shown in the IG-TTD assuming that $CFC-12 = 300$ ppt and $\Delta/\Gamma = 1$ in 1990.

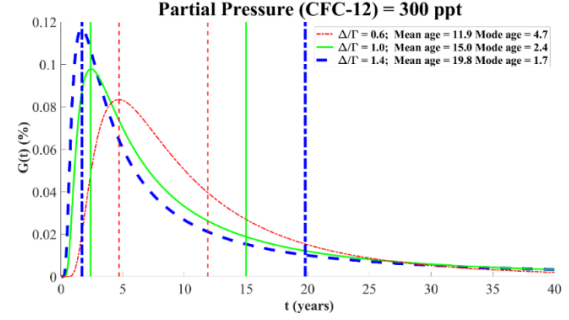
2.3 Determination of the mixing ratio (Δ/Γ):

The atmospheric concentration increased monotonically until mid-1990s for the CFC-12 and is still increasing for the SF₆ (Fig. 2, a). In addition, the mixing ratio (Δ/Γ) also plays a significant role in the calculation of mean-age and mode-age. Under the assumption for a particular tracer concentration, for instance 300 ppt for the CFC-12 in the sampling year 1990, the mean-age increases with the mixing ratio (Δ/Γ), since the “tail” of the Inverse Gaussian Function becomes longer, while the mode-age decreases with the mixing ratio (Δ/Γ) as the “peak” appears earlier (Fig. 2, b).

The significance of mixing ratio to the age calculations is also evident in the observations. The cruise along the A16 section in 2013 (Fig. 3, a) shows that different ratios lead to significant differences in water mass ages, especially when the partial pressures of tracers are low (CFC-12 lower than 50 ppt and SF₆ lower than 0.2 ppt) (Fig. 3, b and c). The mean-ages show relative low values when the ocean is assumed to be a relatively advective ($\Delta/\Gamma < 0.8$). Most mean-ages below 1500 dbar are between ~ 300 and 700 years, with some mean-ages around 20°N even higher than ~ 700 years (although this is close to the detection limit for the corresponding CFC-12 concentrations). In contrast, the mean-ages are generally higher than ~ 700 years with diffusive ($\Delta/\Gamma > 1.4$) assumption (Fig. 3, b). The situation of mode-ages is the opposite. The mode-ages are higher, mostly between ~ 50 and 100 years in the intermediate layer, higher than ~ 100 years in the deep and bottom layer and above ~ 150 years around 20°N under the advective ($\Delta/\Gamma = 0.8$) assumption, while most mode-ages show low values around ~ 50 years under the diffusive ($\Delta/\Gamma = 1.4$) assumption (Fig. 3, c).



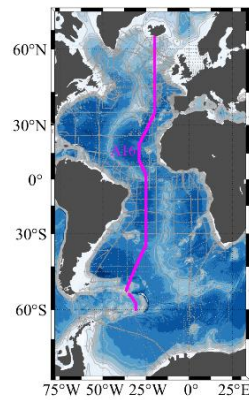
(a)



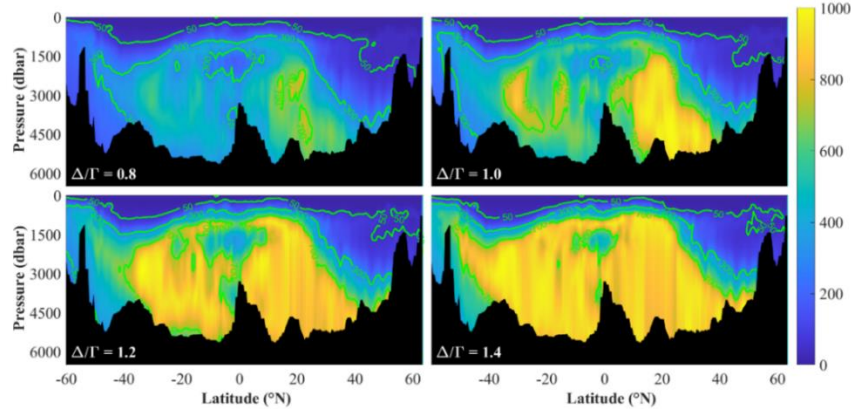
(b)

Figure 2. The relationships between mean-age, mode-age and mixing ratio (Δ/Γ).

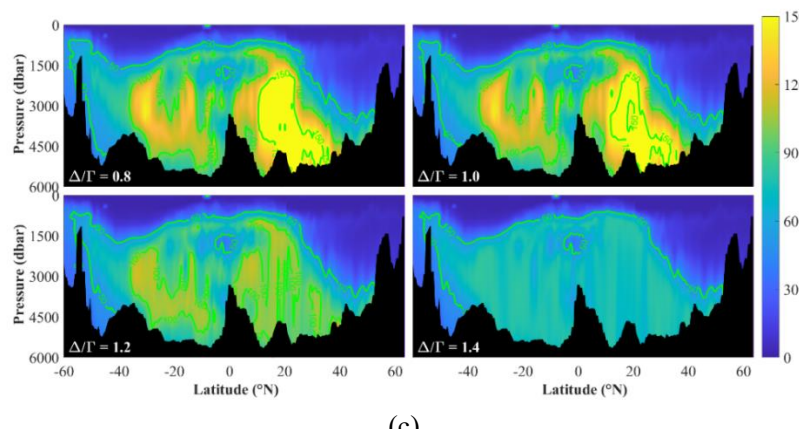
(a) Atmospheric historical partial pressure of transient tracers over time (CFC-12 and SF₆) in the North Hemisphere;
 (b) Relationship between mean-ages and mode-ages under same partial pressure (CFC-12 = 300 ppt) but different mixing ratios (Δ/Γ) in the sampling year 1990.



(a)



(b)



(c)

Figure 3. The A16 section of WOCE/GO-SHIP in 2013 (a) and the distributions of mean-ages (b) and mode-ages (c) with different mixing ratios ($\Delta/\Gamma = 0.8, 1.0, 1.2, 1.4$) based on the GLODAPv2 observational data



145 The determination of the shape of the TTD, i.e. of the mixing ratio (Δ/Γ) if you assume an Inverse Gaussian distribution, is
one of the prerequisites before estimating the ages of water masses. In the specific regions with a small-scale calculation, or
under a typical diffusive or convective situation where the mixing ratio is quite different from 1, a corresponding value of
mixing ratio (Δ/Γ) according to the specific situation is required to obtain the relative accurate water ages (Waugh et al., 2004;
Schneider et al., 2014). However, in most cases the lack of independent tracer data limits the options to empirically estimate
150 of mixing ratios in most areas. In order to calculate the distribution of transient tracers and the ages of water masses over the
Atlantic Ocean, a reasonable assumption is the standard mixing ratio ($\Delta/\Gamma = 1$, Waugh et al., 2004; Stanley et al., 2012;
Thomas et al., 2020) for the general calculations (Schneider et al., 2010; Huhn et al., 2013; Stöven and Tanhua, 2014). In this
study, the standard mixing ratio ($\Delta/\Gamma = 1$) is followed to estimate the mean-ages and mode-ages of water masses in the
Atlantic Ocean.

155 **3 Results: Ages of water masses in the Atlantic Ocean**

This work builds on the study by Liu and Tanhua, (2021) that estimated the physical extension of water masses in the Atlantic
Ocean. We follow the division of vertical layers and distributions of water masses presented by Liu and Tanhua (2021), but
now focus on the transient tracers and water mass ages. Three hydrographic sections are selected from the WOCE/GO-SHIP
160 sections in this work to represent the mean-ages of the main water masses (Table 1). The A16 sections in 2013 (Expo-code
33RO20130803 and 33RO20131223) show the meridional distribution across the whole Atlantic Ocean, while the A05 section
in 2010 (Expo-code 74DI20100106) and A10 section in 2011 (Expo-code 33RO20110926) show the zonal distributions in the
North and South Atlantic Ocean respectively (Fig. 4). The partial pressures of CFC-12 and SF₆ along the above sections are
shown in Fig. 4 (Only CFC-12 data are displayed along A05 section due to the lack of SF₆ data in this section). Both tracers
show similar distributions with high values in the shallow layers, and a general decrease with increasing pressure.

165 **Table 1: Expo-code, Ship, Chief scientists and PI of transient tracers for the selected hydrographic cruises to the
Atlantic Ocean showed as sections in this study**

WOCE/GO-SHIP section	Year	Expo-code	Ship	Chief Scientist	PI of transient tracers
A16N	2013	33RO20130803	Ronald H. Brown	John Bullister & Molly Baringer	John Bullister
A16S	2013	33RO20131223	Ronald H. Brown	Rik Wanninkhof	John Bullister
A05	2010	74DI20100106	Discovery	Brian King	Marie-José Messias
A10	2011	33RO20110926	Ronald H. Brown	Molly Baringer	John Bullister

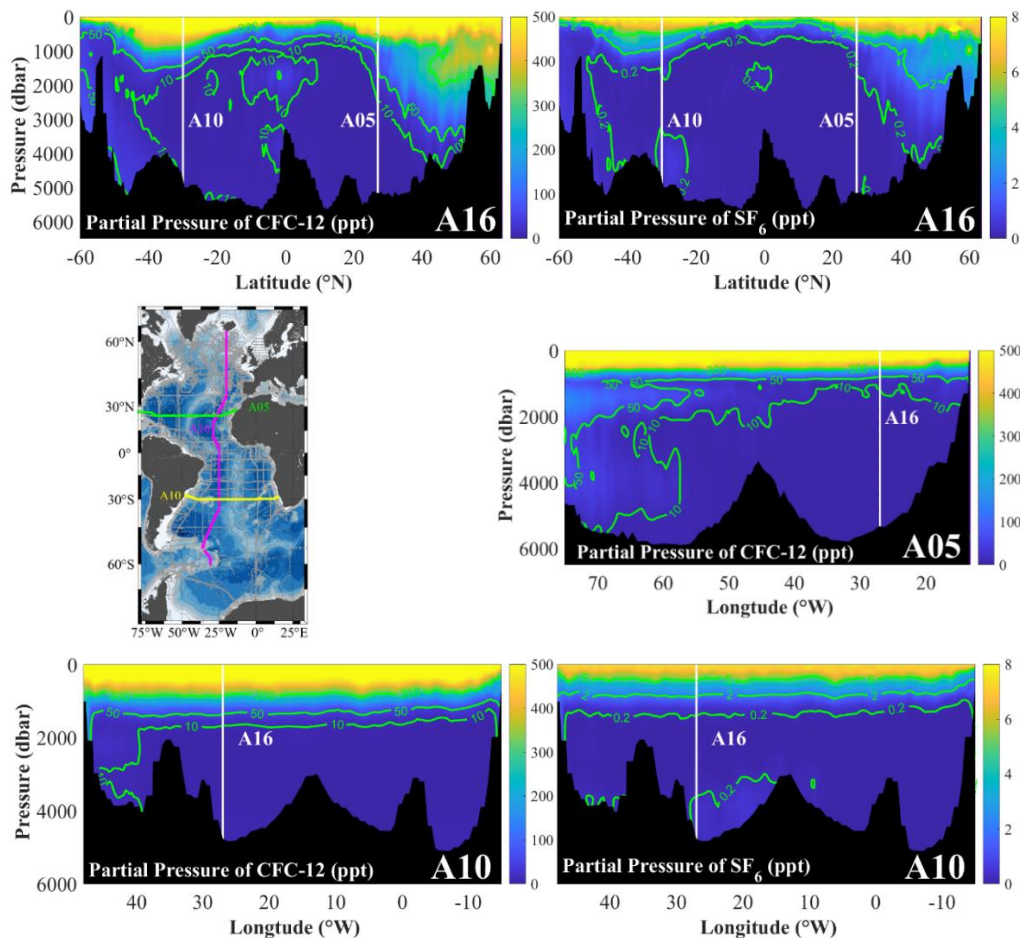


Figure 4. Map of three selected WOCE/GO-SHIP sections to represent the ages of the main water masses in the Atlantic Ocean (middle left) and partial pressures of CFC-12 and SF₆ along the three selected sections.

In this study, CFC-12 is used to estimate water mass ages when the partial pressures of CFC-12 are lower than 450 ppt, while 170 the SF₆ is used when the partial pressures of CFC-12 are higher than 450 ppt according to Tanhua et al., (2008). The distributions of partial pressures mean that the upper layer have the lowest mean-ages within ~100 years and mode-ages within ~30 years (Fig. 5). The distributions of mean-ages and mode-ages also show spatial differences in the horizontal direction. Relatively low ages are found in the high latitude regions (Fig. 5, a and b). This indicates that the deep water masses are newly 175 formed here, and thus have low ages. In the region between 20 and 40 °N, the mean-age reaches the peak value up to ~1000 years and the mode-age up to ~150 years, suggesting the sluggish water exchange and long residence time of old water masses. In the zonal direction, both mean-ages and mode-ages are significantly lower in the west in the general region below 1500m dbar, suggesting that these regions are better ventilated due to the western boundary current (Fig. 5 c to f).

In the analysis of water mass ages in each layer, maps with mean-ages and mode-ages in each station are firstly presented as a 180 qualitative overview. The mean values of the ages at the core pressure of each water mass are plotted at certain station. In addition, the quantitative calculations are made along the three selected sections to represent the distributions of water mass ages in detail and estimate the impacts from currents and mixing.

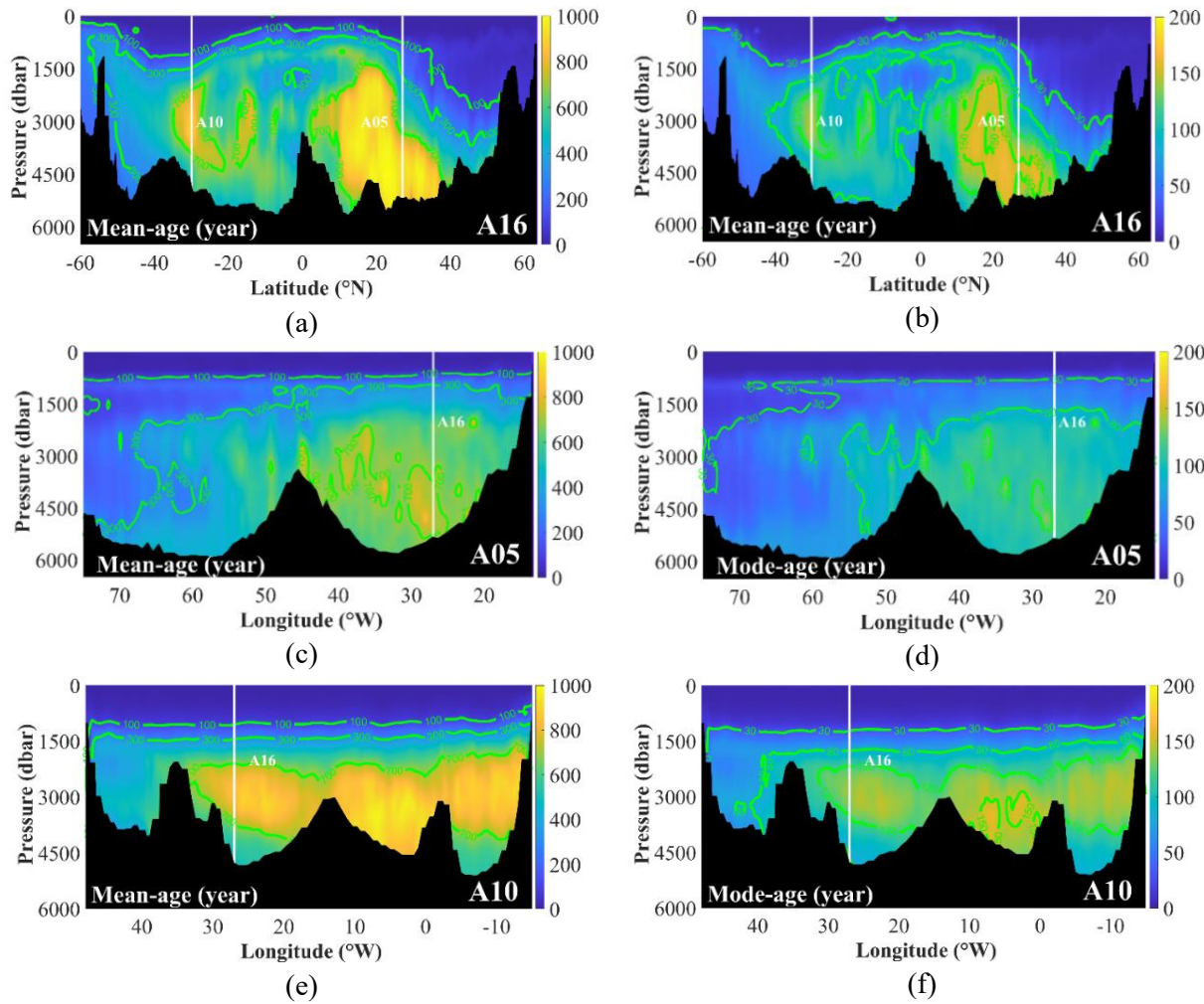


Figure 5. Mean-ages and Mode-ages along the three selected WOCE/GO-SHIP sections

3.1 The upper layer

The spreading of central waters can be traced by the distributions of ages. After leaving their formation areas in the mid-latitude regions, the West North Atlantic Central Water (WNACW) and West South Atlantic Central Water (WSACW) spread

185 generally in zonal direction towards the formation areas of the East North Atlantic Central Water (ENACW) and East South Atlantic Central Water (ESACW) with Azores Current and South Atlantic Current, respectively (Fig. 6, a). The mean-ages show that the “mixed” age of all the compositions in the western central waters is ~50 years (Fig. 6, b and Fig. 7). When focusing on the main body of WNACW and WSACW, the mode-ages show that the advective time-scale is ~15 years for both water masses (i.e. Both WNACW and WSACW take ~15 years from the formation area to the equator, Fig. 6, c and Fig. 7).

190 At greater depths, the ENACW and ESACW are transported from their formation areas and spread with the main currents towards the equator (Fig. 6, a). In the northern hemisphere, the ENACW spreads southward with the Canaries Current, while



the ESACW in the southern hemisphere is transported northward with the Benguela Current and the South Equatorial Current. The difference in mean-age is \sim 100 years between the formation areas and the equatorial region (Fig. 6, b and Fig. 7). The mode-ages indicate that the main body of ENACW and ESACW takes approximately 30 years to be transported from formation 195 areas to the equator (Fig. 6, c and Fig. 7). The central waters occupy the upper layer above the neutral density isoline of 27.10 kg m^{-3} . The core pressures of western and eastern central waters are around the neutral density (γ) of 26.5 and 26.9 kg m^{-3} respectively (Liu and Tanhua, 2021). The ages of central waters at their core neutral densities are shown in Fig. 6. The eastern 200 central waters have mean-ages of up to approximately 100 years and mode-ages up to approximately 30 years, while the western central waters are younger with ages of \sim 50 years and \sim 15 years respectively (Fig. 6). The relatively low ages in the upper layer indicate that these water masses are newly formed. In the meridional direction along the A16 section, both mean-ages and mode-ages show low values of around 20 years in the mid-latitude regions that are close to the formation areas of central waters (Fig. 6 and Fig. 7). In contrast, the ages are higher (\sim 100 years for mean-age and \sim 30 years for mode-ages) in the tropical region. In the zonal direction, the ages in the eastern basin are slightly higher than in the western basin for the central waters, but the difference is only within \sim 10 years for both mean-ages and mode-ages, indicating that the influence 205 from western boundary current is not significant in the upper layer. (Fig 7).

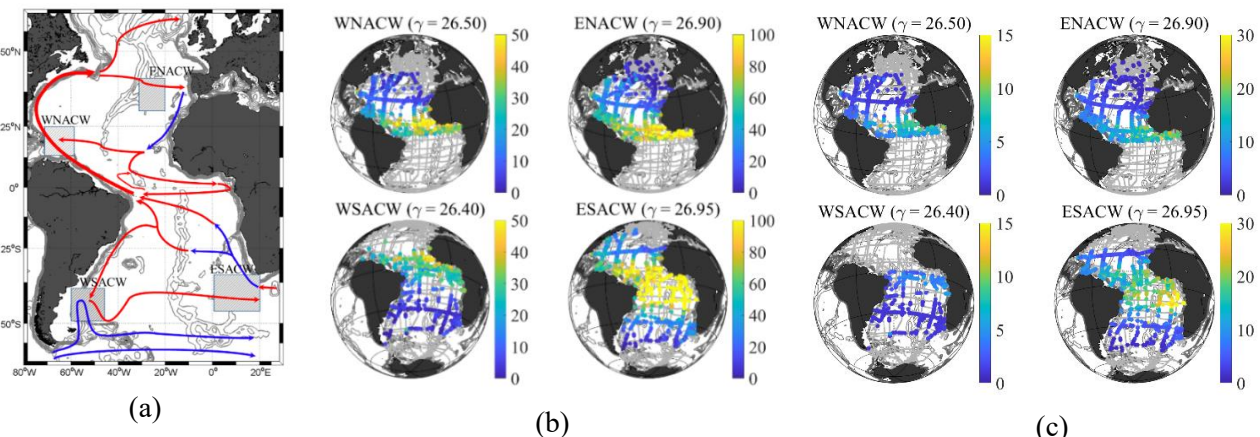


Figure 6. Ages of central water masses in the Atlantic Ocean.

(a) The main currents in the upper layer with warm (red) and cold (blue) currents and the approximate formation areas (rectangular shadows) of central water masses.

(b) The mean- and (c) mode-ages of central water masses at their core neutral densities (kg m^{-3}). The colored dots show the ages in each station. The grey dots show all the GLODAPv2 stations that have less than 20% contribution of the water mass in question or lack of transient-tracer data.

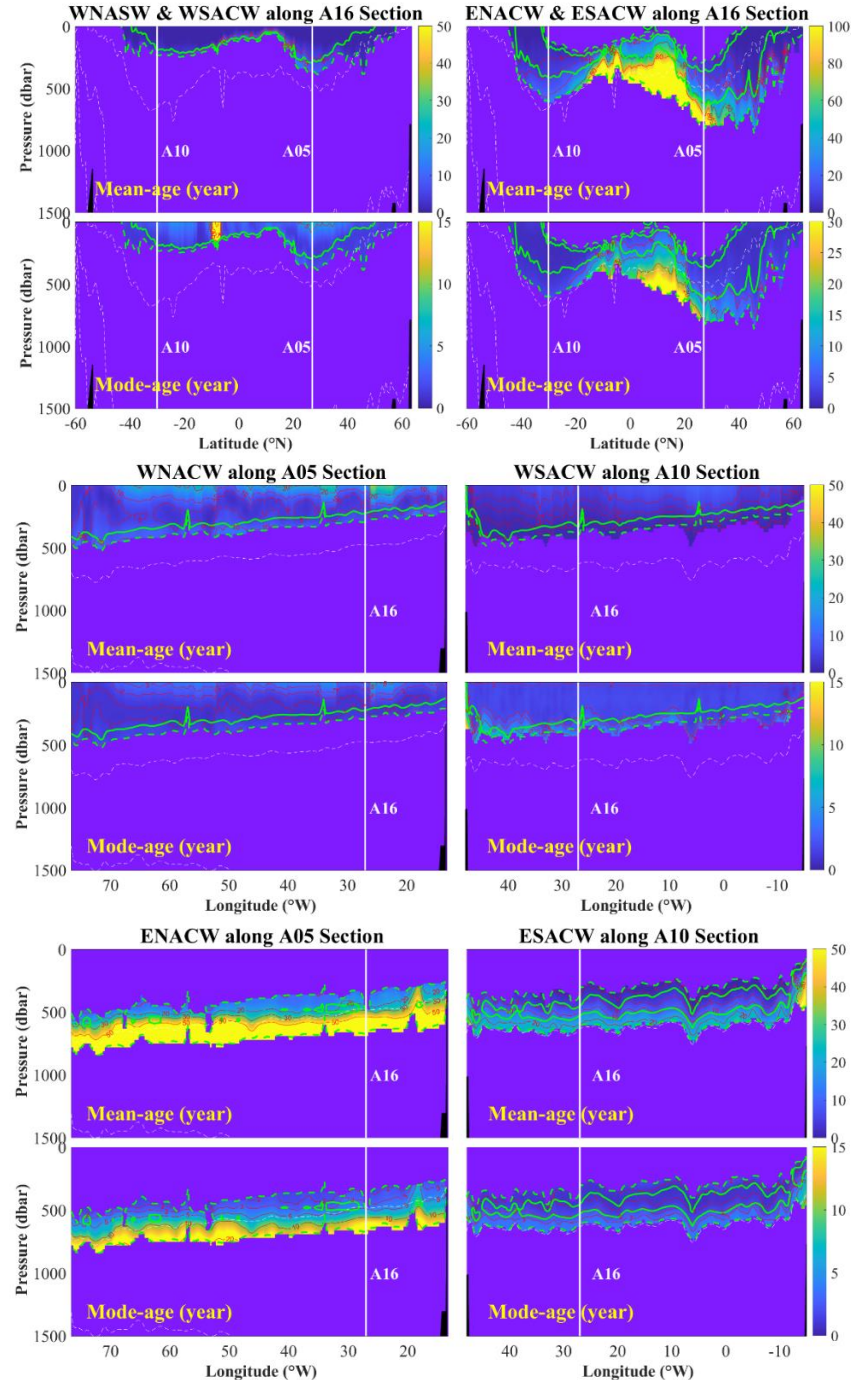


Figure 7. The mean- and mode-ages of central waters along the three sections for the upper 1500 dbar. The solid green isolines show the 50% fractions of water masses and the dashed green lines show the 20 % fractions. The purple blank indicates less than 20% contribution from central waters. White vertical lines show cross overs with other sections and dashed white lines show vertical boundaries of layers (neutral density at 27.10, 27.90 and 28.10 kg m^{-3}).



3.2 The Intermediate Layer

Three main water masses belong to the intermediate layer (γ between 27.10 and 27.90 kg m^{-3}), including the Antarctic Intermediate Water (AAIW), the Subarctic Intermediate Water (SAIW) and the Mediterranean Water (MW). The ages of SAIW 210 are not displayed in this study due to the lack of tracer data with a complete section through in the distribution region of this water mass.

Antarctic Intermediate Water (AAIW): The AAIW spreads from the formation area between 40 and 50 °S northward to approximately 30 °N along the Western Boundary Current (WBC) (Fig. 8, a). The northward flow of this water mass is part of the Atlantic western boundary current system (Talley, 1996) and the upper limb of AMOC (Kirchner et al., 2009).

215 Compared to the central waters, AAIW has significantly higher ages. In principle, the AAIW is supposed to get higher ages towards the north. In the meridional direction, the mean- and mode-ages increase from 0 to ~300 years and ~80 years from formation area to the equator, and further increase up to ~400 years and ~100 years respectively to 20 °N (Fig. 8 and 9). However, both ages decrease instead and approach even towards 0 in the further north region between 20 °N and 30 °N (Fig 220 8, b and c), giving the impression of the AAIW being younger in the north Atlantic Ocean. The reason for the above result is the intervention from surrounding water masses. The maximum distance of AAIW to the north can reach 30 °N, but between 20 °N and 30 °N, this water mass mixes with the ENACW and upper NADW (Fig 7, a, Fig. 9, a and Fig. 11, a), which originates from the Labrador Sea Water (LSW, Liu and Tanhua, 2021). Both ENACW and upper NADW are newly formed in this region, so the “mixed” AAIW obtains younger ages. Age differences are also found in the zonal direction. In better ventilated western 225 basins, the AAIW transports northward with the western boundary current (WBC), so the mean- and mode-ages are lower. By contrast, the ages are significantly higher in the eastern basins with poor ventilation. The mean-ages reach ~400 years and the mode-ages are up to ~100 years in the east between 0 and 20 °S (Fig. 8, b and c). The mean- and mode-ages along the A05 section also show the zonal difference (Fig. 9, b). In the eastern basin (east of the Mid-Atlantic-Ridge, MAR), the mean-age and mode-age appears up to ~400 and ~80 years respectively, in contrast only ~200 years and ~50 years in the west. This 230 distribution confirms that the AAIW is transported by the WBC and takes a longer time to cross the MAR. Generally lower ages are found along the A10 Section in contrast to the A05 Section due to closer distance to the formation area of AAIW (Fig. 9, c). Similar zonal difference exists with mean-ages of ~50 years in the west ~100 years in the east and mode-age of ~10 years in the west and ~ 20 years in the east.

Both mean- and mode-ages of AAIW also show differences in the vertical direction due to the mixing with other water masses. At the shallow boundary to the upper layer, the AAIW mixes with “younger” eastern central waters. At the lower boundary to 235 the deep and overflow layer, the northward flowing AAIW mixes with the southward flowing upper NADW. Along the A10 section, the upper NADW has experienced long spreading times and obtained a high mean-age of ~600 years and a mode-age of ~80 years (Fig. 11). As a result, the “mixed” ages between AAIW and upper NADW (~300 years for mean-age and ~60 years for mode-age) are relative high at the border compared to the ages at core of AAIW (~100 years for mean-age and ~20 years for mode-age, Fig 9, c). The situation is the opposite along the A05 section: The AAIW is old in the north Atlantic, while 240 the upper NADW here is still relatively young. The “mixed” mean-age is ~200 years and mode-age is ~50 years in contrast to ~300 years for the mean-age and ~60 years for mode-age at the core of AAIW (Fig 9, b). This result is consistent with the ages of NADW in the next section.



245 **Mediterranean Water (MW):** The MW is referred to as the product of the Mediterranean Overflow Water (MOW) that flows across the Strait of Gibraltar and mixes with the ENACW (Liu and Tanhua, 2021). This water mass is formed in the Gulf of Cadiz where the MOW exits the Strait of Gibraltar as a deep current and turns into two branches (Fig 8, a). The northward branch spreads into the West European Basin until 50 °N, while the westward branch spreads across the MAR into the west basin of the North Atlantic Ocean (Price et al., 1993; Carracedo et al., 2016).

250 The spreading of MW can also be traced by the transient tracers (Fig 9, a), in addition to the water mass variables that goes into the OMP analysis (Liu and Tanhua, 2021). The ages of MW have an increasing trend towards the south (Fig. 8, b and c). The northward flow spreads faster so the mean-age is ~100 years and the mode-age is ~ 20 years at 50 °N. In contrast, the southward flow shows a higher mean-age of ~400 years and mode-age of ~100 years at 25 °N along the A05 Section (Fig 9, b). In the zonal direction, the ages decrease to the west (Fig 9, b), since the fraction of MW is only between 20% and 30% along this section (green dash contour lines in Fig 9, b), and is therefore influenced by the lower ages from the NADW.

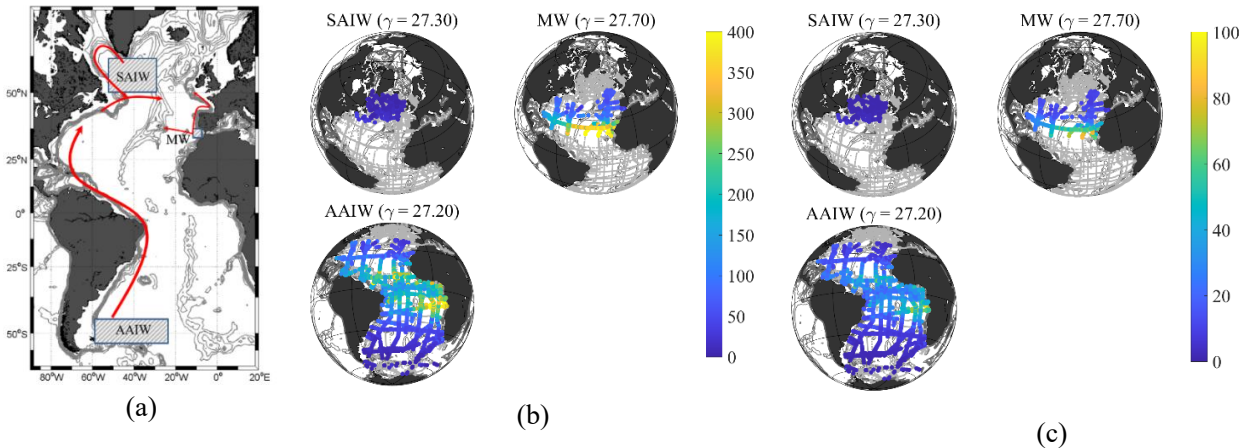


Figure 8. Ages of intermediate water masses in the Atlantic Ocean.

(a) Main currents in the intermediate layer. The currents (arrows) and the formation areas (rectangular shadows) of water masses in the intermediate layer.

(b) The mean- and (c) mode-ages of intermediate water masses at their core neutral densities (kg m^{-3}). The colored dots show the ages in each station. The grey dots show all the GLODAPv2 stations that have less than 20% contribution of the water mass in question or lack of transient-tracer data.

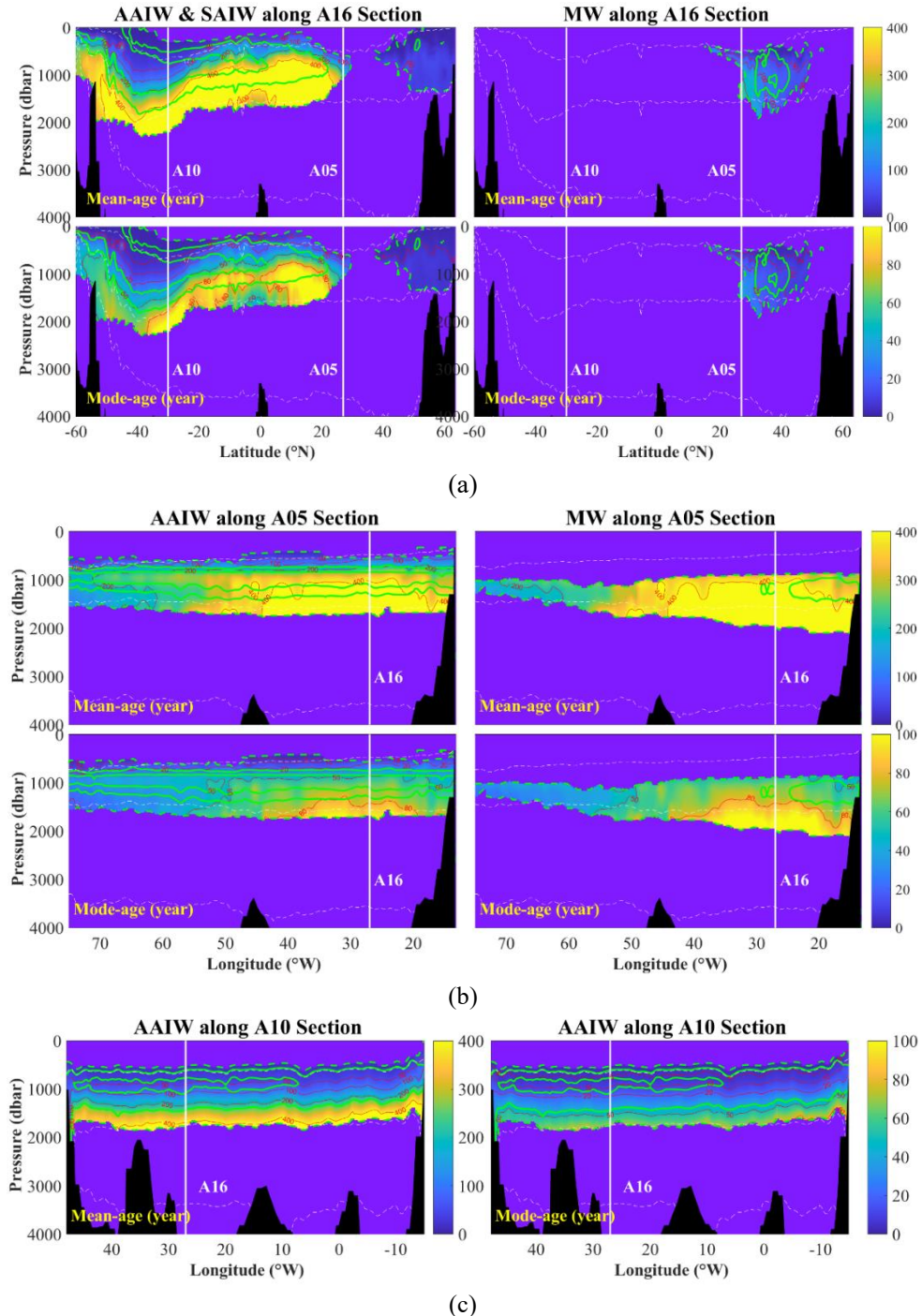


Figure 9. Mean- and mode-ages of intermediate water masses along the three sections for the upper 4000 dbar. The solid green isolines show the 50% fractions of water masses and the dashed green lines show the 20 % fractions. The purple blank indicates less than 20% contribution from intermediate water mass. White vertical lines show cross overs with other sections and dashed white lines show vertical boundaries of density layers (neutral density at 27.10, 27.90 and 28.10 kg m^{-3}).



255 3.3 Deep and Overflow Layer

The North Atlantic Deep Water (NADW), including its upper and lower portions, dominates the deep and overflow layer (γ between 27.90 and 28.10 kg m^{-3}) of the Atlantic Ocean. This water mass is formed in the high latitude region in the North Atlantic and spreads southward at pressures between 2000 and 4000 dbar until it meets AAIW and AABW in the Antarctic Circum-polar Current (ACC) region. The southward spreading pathway is along the Deep Western Boundary Current (DWBC, 260 Fig. 10, a). Meanwhile, the NADW also extends eastward with the eddies and finally covers the deep and overflow layer (Dickson and Brown, 1994).

Upper and lower North Atlantic Deep Water (NADW): The NADW is a water mass that is transported far southward from its formation area, with a mean-age of \sim 600 years (Fig. 11, b) and mode-age of \sim 100 years (Fig. 10, c) at the southern limb in the Antarctic Circum-polar Current (ACC) region. The increasing ages during the pathway to the south is shown along the A16 section (Fig. 11, a). After leaving the formation area, the mean- and mode-ages increase \sim 200 and \sim 20 years respectively from 265 60 $^{\circ}$ N to 40 $^{\circ}$ N. Afterwards, a sharply increase in both ages appear in the region between 30 $^{\circ}$ N and 10 $^{\circ}$ N. In this interval, the highest value of mean-age reaches \sim 1000 years and the mode-age is up to \sim 150 years. This is because the A16 section at this 270 latitude range passed through the east part of the Atlantic Ocean (east of MAR) and the distance from the Deep Western Boundary Current (DWBC, Fig. 4 and Fig. 10, a) was high. High ages in this region are due to the sluggish water exchange over ridge. This result can also be confirmed by the observation along the A05 Section (Fig. 11, b): The NADW near the DWBC region has a low mean-age of \sim 200 years and mode-age of \sim 40 years, while the ages are up to \sim 600 years and \sim 100 years east of the MAR. After passing the equator, when the A16 section returns to the west of the MAR, the mean-ages of 275 NADW are \sim 400 years and the mode-ages are \sim 80 years in the latitude range between 0 and 20 $^{\circ}$ S, which further increase to \sim 600 (mean-ages) and \sim 100 (mode-ages) years along the pathway southward until 40 $^{\circ}$ S. In the ACC region between 40 $^{\circ}$ S and 60 $^{\circ}$ S, the mean- and mode-ages of upper and lower NADW decrease to \sim 400 and \sim 80 years respectively. Similar to the 280 situation of AAIW in the north Atlantic, this is also the result of mixing with newly formed AAIW and AABW. The spreading of NADW in the zonal direction is slower eastward, so the ages are generally higher in the eastern basin of the Atlantic Ocean (Fig. 10, b and c). The tracer data along the A05 and A10 sections also reflect the above result. In the A05 section, the mean-ages are \sim 200 years in the west and \sim 600 or even \sim 800 years in the east, and the mode-ages show \sim 50 years in the west and \sim 100 to \sim 120 years in the east (Fig. 11, b). In the A10 section, the mean-ages are \sim 400 years in the west and \sim 800 years in the east and the mode-ages are \sim 80 years in the west and \sim 120 years in the east (Fig. 11, c).

In the vertical direction, the upper NADW mixes with the AAIW from above and the lower NADW mixes with the AABW from below. As the NADW is transported in the opposite direction to these two water masses, the “mixed” ages in the north, 285 which is closer to the formation area of NADW, are higher than the age at the core density of NADW, while the opposite situation exists when spreading to south. After entering the ACC region, both mean-age and mode-age even decrease since the fractions of newly formed AAIW and AABW are high.

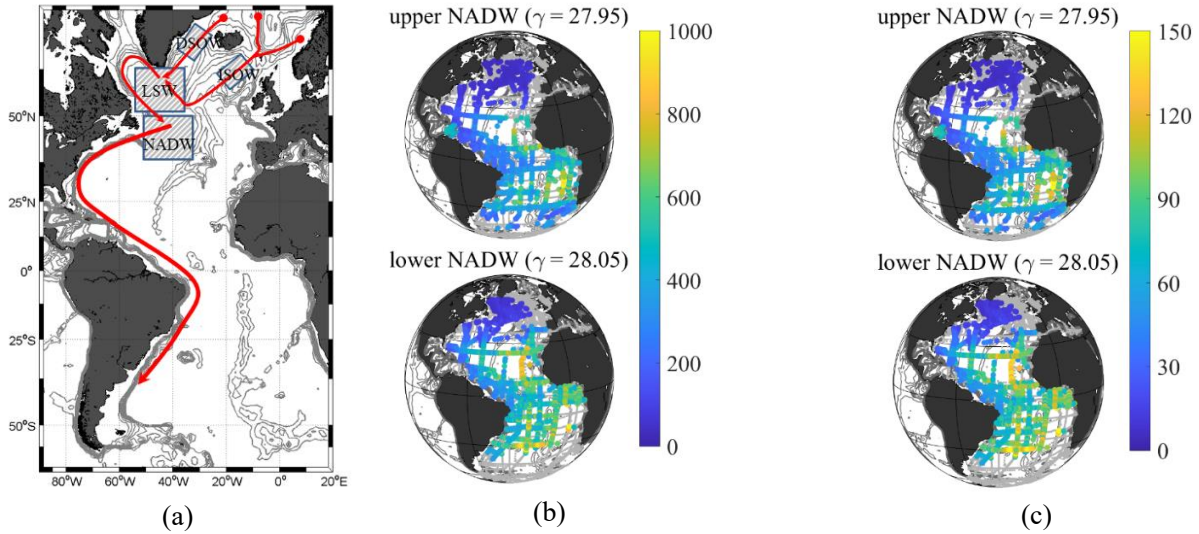


Figure 10. Ages of upper and lower NADW in the Atlantic Ocean.

(a) Main currents in the deep and overflow layer. The currents (arrows) and the formation areas (rectangular shadows) of water masses in the deep and overflow layer.

(b) The mean- and (c) mode-ages of upper and lower NADW at their core neutral densities (kg m^{-3}). The colored dots show the ages in each station. The grey dots show all the GLODAPv2 stations that have less than 20% contribution of the water mass in question or lack of transient-tracer data.

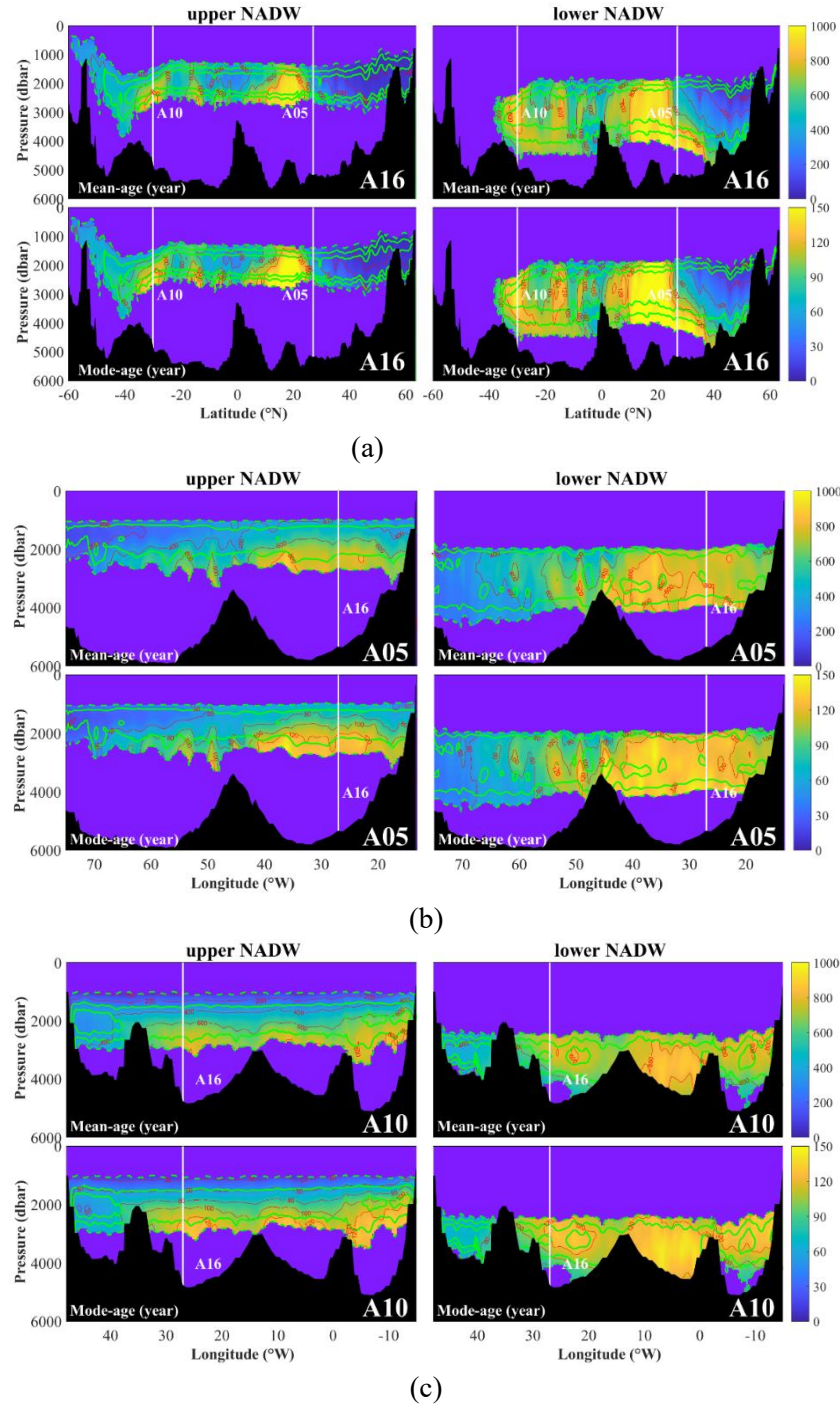


Figure 11. Mean- and mode ages of upper and lower NADW along the A16 (a), A05 (b) and A10 (c) section lines. The green contour lines show fractions of water masses in 50 % and the dashed green lines show the 20 % fractions. The purple blank indicates less than 20% contribution from NADW. The white vertical lines show cross overs with other section lines.



3.4 Bottom Layer

The bottom layer is noticed already by Wüst, (1933) as it is filled with water from the south. Sverdrup, (1940) further pointed out the role of ACC plays in the formation and spreading of Antarctic Bottom Water (AABW). On this basis, Mantyla and 290 Reid, (1983) elaborated that the most original dense bottom water is restricted near the Antarctic region by topography and the northward flow of bottom water is the mixture of original dense water and the overlying warm water. Gordon and Huber (1990) and Orsi et al., (1999) illustrated that the pathway of AABW to the north is through the Drake Passage sill into the Argentina and Brazilian Basin (Fig. 12, a). In the Atlantic Ocean, the AABW dominates the bottom layer ($\gamma > 28.10 \text{ kg m}^{-3}$), which 295 originates from the Weddell Sea and spreads to the north. After passing the equator, the AABW is redefined as Northeast Atlantic Bottom Water (NEABW, Liu and Tanhua, 2021).

Antarctic Bottom Water (AABW) & Northeast Atlantic Bottom Water (NEABW): The transport of bottom water is a long process going from the south towards the north. In the meridional direction, the AABW is transported towards the equator with a mean-age of ~ 600 years and mode-age of ~ 100 years at the equator, and further northward as NEABW to 40°N with a mean-age of ~ 1000 years and mode-age of ~ 150 years (Fig. 12, b and c). Combined with the A16 Section, more specific 300 segments/details can be seen. In the early stage from the surface of Weddell Sea to the bottom (below the pressure 4000 dbar) at 40°S , the mean-age of AABW is ~ 300 years and mode-age is ~ 50 years. In the range between 10 and 30°S , high values of ~ 800 years (mean-age) and ~ 120 years (mode-age) appear due to the mixing with the lower NADW with high ages (Fig. 13, a). After passing the equator, the redefined NEABW contains a mean-age up to ~ 1000 years and mode-age up to ~ 150 years 305 at 40°N , indicating that the bottom water, including the AABW and NEABW, takes about 150 years (mode-age) for the transport from the formation area (Weddell Sea) to 40°N . North of 40°N , the ages decrease due to the mixing with newly 310 formed lower NADW in this region (Fig. 12, b and c, Fig. 13, a). The distribution of mean- and mode-ages also show a difference in the zonal direction. As shown in Fig. 12 b and c, the general age distribution presents a trend with lower ages in the west, and higher in the east. Along the A10 section at 30°S , the AABW has a mean-age of ~ 400 in the west and ~ 600 years in the east, whereas the mode-age is ~ 50 in the west and ~ 100 in the east. A similar situation is recorded along the A05 section; 315 the mean-age of NEABW is ~ 600 years in the west and ~ 800 years in the east, whereas the mode-age is ~ 80 years in the west and between ~ 120 years in the east (Fig. 13, b). An additional factor that affects the age distributions is the mixing between AABW and NADW. In the south hemisphere, both ages are relatively low (~ 400 years for mean-age and ~ 80 years for mode-age) at the pressures below 4000 dbar, where the AABW has a fraction higher than 50%, while the ages are significantly higher when the AABW mixes with lower NADW at pressure of ~ 3000 dbar, especially in the region between 0 and 10°W , the mean-age reaches up to ~ 800 years and the mode-age is ~ 120 years. This is because the “old” NADW takes up a fraction for more than 320 50% to 80%. The situation in the north hemisphere is the opposite, the ages of NEABW are higher in the bottom layer below 4000 dbar but lower in the deep layer at 3000 dbar due to the mixing with the young NADW. In the western basin, the mean-age is ~ 600 years and mode-age is ~ 80 years in the bottom, while ~ 400 years and ~ 50 years when mixes with NADW. Similar in the east basin, the mean-age is ~ 800 years and mode-age is ~ 120 years below 4000 dbar, while ~ 600 years and ~ 100 years at 3000 dbar (Fig. 13, b).

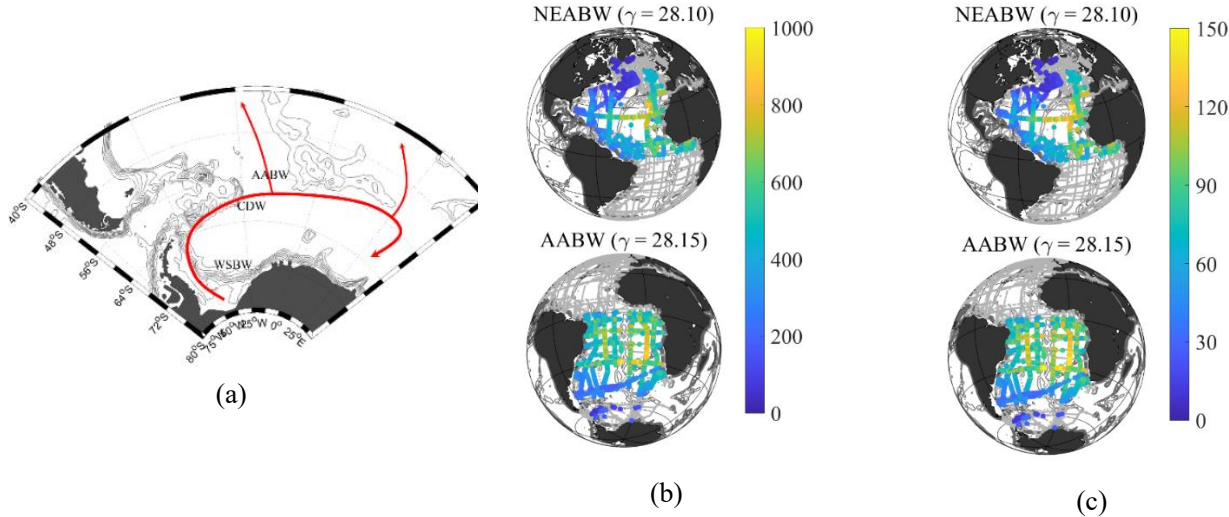


Figure 12. Ages of bottom water masses in the Atlantic Ocean.

(a) Main currents in the bottom layer. The currents (arrows) and the formation areas (rectangular shadows) of water masses in the deep and overflow layer.

(b) The mean- and (c) mode-ages of bottom water masses at their core neutral densities (kg m^{-3}). The colored dots show the ages in each station. The grey dots show all the GLODAPv2 stations that have less than 20% contribution of the water mass in question or lack of transient-tracer data.

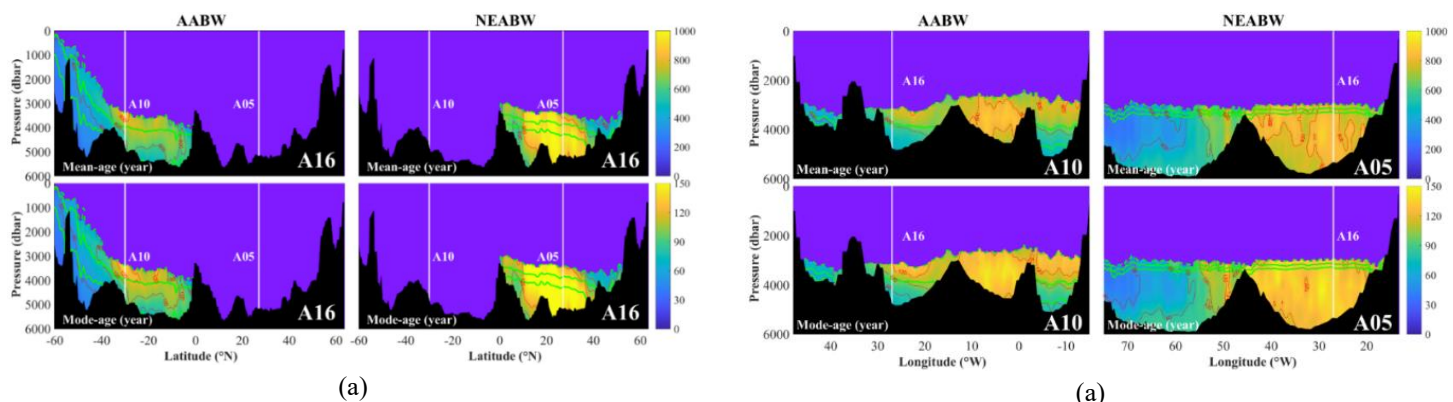


Figure 13. Mean-ages of AABW and NEABW along the A16 (a), A05 and A10 (b) section lines.

The green contour lines show fractions of water masses in 50 and the dashed green lines show the 20 % fractions. The purple blank indicates less than 20% contribution from bottom water masses. The white vertical lines show cross overs with other section lines.



4 The application of water mass ages in estimating the oxygen utilization rate (OUR)

The oxygen concentration in seawater under steady state is maintained by the balance of supply from oxygen-rich surface water and consumption by the respiration of organic matter. The Apparent Oxygen Utilization (AOU) shows the accumulated oxygen consumption in a water mass since isolated from the atmosphere, and is defined as the difference between saturated and measured oxygen concentration (i.e. $\text{AOU} = \text{Oxy}_{\text{saturated}} - \text{Oxy}_{\text{measured}}$, Redfield, 1942; Redfield et al., 1963; Pytkowicz, 1971). The Oxygen Utilization Rate OUR ($\mu\text{mol kg}^{-1} \text{yr}^{-1}$) can be calculated from AOU and water mass age and shows the integrated oxygen utilization rate (oxidation rate) during the pathway of a water mass from surface of the formation area to the sampling location (Jenkins, 1987; Doney and Bullister, 1992; Sonnerup et al., 2013). In addition, the OUR is also an important indicator in characterizing the combination of ventilation and respiration of the interior ocean (Koeve and Kähler, 2016; Thomas et al., 2020).

The true, or local OUR is difficult to estimate, and the main difficulty focuses on the determination of the “true” water mass age since the seawater comes from different pathways due to the mixing in the ocean interior (Tomczak, 1999; Koeve and Kähler, 2016). Researchers have tried a variety of ways to define the age of a water mass. For instance, the tracer-age (CFC age) is used in Karstensen et al., (2008), while the mean-age (partial pressure ages) is used in Sonnerup et al., (2015) in estimating the “integrated” water mass age that effects the oxygen consumption. As described in Section 2.2, the mean-age represents the average of all the parts in one water sample, so the OUR calculated from mean-age is a “mixed” value of all the contributing water masses in the sample. In the steady state, the mean-age can reflect the “mixed” or “integrated” OUR objectively. However, when we are labelling a specific wide-spread water mass and investigating the transport time from formation area, this water mass is often mixed with the surrounding water masses, so the mean-age reflects the “mixed” OUR of the mixture instead of the original labelling water mass. In this case, the mode-age is a better choice, because it describes the dominant time-scale a specific water mass takes from surface of formation area to the pressure of sampling place. In other words, the mode age is closer to the transport time of the original water mass and the OUR calculated from the mode-age might be a reasonable representation of the average OUR during the transport to the sampling location. In this section, we focus on the wide-spread water masses in the Atlantic Ocean and the mode-age is used to calculate the OUR during the active transport of wide-spread water masses.

Water masses with mode-ages larger than ~50 years in some parts of their distribution, including the AAIW, NADW, AABW and NEABW in the Atlantic Ocean, are defined here as wide-spread water masses. The transports of these wide-spread water masses are significantly influenced by the currents and topography. Therefore, their mode-age shows regional differences. Such differences also exist in DO and AOU, and lead to the spatial differences in OUR, especially between the eastern and western basins (Fig. 14). In the meridional direction, the mode-age increases with the distance from formation area. In the zonal direction, significant differences exist between the east and west of MAR. The wide-spread water masses generally have lower mode-ages in the western basin, which is better ventilated by the WBC and the DWBC (Fig. 14, left). In addition, surface oxygen-rich water is transported by these water masses to the deeper layers and are gradually consumed during the path-way. As a result, the DO is highest in the formation area and decreases with the distance. Meanwhile, the western basin displays higher DO due to the better ventilation (Fig. 14, middle left). The OUR shows a similar distribution to DO indicating that higher oxygen consumption rate, or oxidation rate is co-located with the regions with high oxygen concentration. At the same time, Fig. 14 also shows that the OUR approaches 0 when the mode-age is larger than ~50 years.

In the intermediate layer, the AAIW show low mode-ages, high DO and low AOU in the formation area near the Antarctic region. During the northward transport between 40 °S and 20 °N, the mode-ages increase and the DOs decrease with distance from the formation area (Fig. 14, upper panel). In general, the mode-ages are lower in the west, while the zonal difference for



DOs are not significant except for some regions in the eastern basins. The mode-ages are mostly between ~60 and ~90 years and reaches up to ~120 years in the poor ventilated eastern basin. The DOs are between 160 and 220 $\mu\text{mol kg}^{-1}$ in the south hemisphere and mostly between 100 and 160 $\mu\text{mol kg}^{-1}$ in the north hemisphere. The OURs in the Antarctic region obtain the 365 highest value in the latitude region between 20 and 40 $^{\circ}\text{S}$ and decrease on the pathway to the north until 20 $^{\circ}\text{N}$.

In the deep and overflow layer, the NADW is newly formed in the high north latitude. In most regions covered by the NADW between 30 $^{\circ}\text{N}$ and 40 $^{\circ}\text{S}$, the differences between west and east exist with obvious low mode-age and AOU (high DO) and in the west, where is well ventilated by the DWBC (Fig. 14). The mode-age is between ~30 and ~60 years in the west and between ~90 and ~150 years in the east. The AOU is lower in the west and higher in the east. The OUR, which shows the opposite 370 distribution as the AOU in the zonal direction, obtains the highest value in the formation area of NADW, maintains relative higher in the west along the DWBC region and shows a lower value in the eastern basin.

The bottom layer is occupied by the AABW and NEABW in the south and north hemisphere respectively. The AABW is formed in the Antarctic region with an original mode-age lower than ~30 years and increases on the way to the north. Similar 375 to the AAIW and NADW, the western basin is better ventilated, therefore the mode-ages are lower in the west at the same latitude (Fig. 14, lower panel). In contrast to the AAIW and NADW, the AABW obtains relative lower DOs and higher AOU when formed (see also Fig. 15, b). In the western basin of the South Atlantic, the DOs decrease to 220 $\mu\text{mol kg}^{-1}$ and the AOU increase to 130 $\mu\text{mol kg}^{-1}$ on the pathway, while in the eastern basin, the DOs are 240 $\mu\text{mol kg}^{-1}$ and the AOU are 110 $\mu\text{mol kg}^{-1}$. This is because the eastern basin is more influenced by the relative oxygen-rich NADW from the north. Similarly, the 380 DOs and AOU of NEABW in the North Atlantic also show similar states to the NADW. In west regions ventilated by the DWBC, the DOs reach the values of higher than 260 $\mu\text{mol kg}^{-1}$ and AOU is lower than 70 $\mu\text{mol kg}^{-1}$. This result can also be confirmed in Figure 15. Although the distributions of DOs and AOU are more complex in the bottom layer, the OURs still match the distribution of mode-ages. The highest OURs appears in the formation area near the Antarctic region with values higher than 4 $\mu\text{mol kg}^{-1} \text{yr}^{-1}$. In the western Atlantic region with low mode-ages, the OURs show relative higher values (> between 1 and 3 $\mu\text{mol kg}^{-1} \text{yr}^{-1}$) and low value (below 1 $\mu\text{mol kg}^{-1} \text{yr}^{-1}$) in the east (Fig. 14, lower panel).

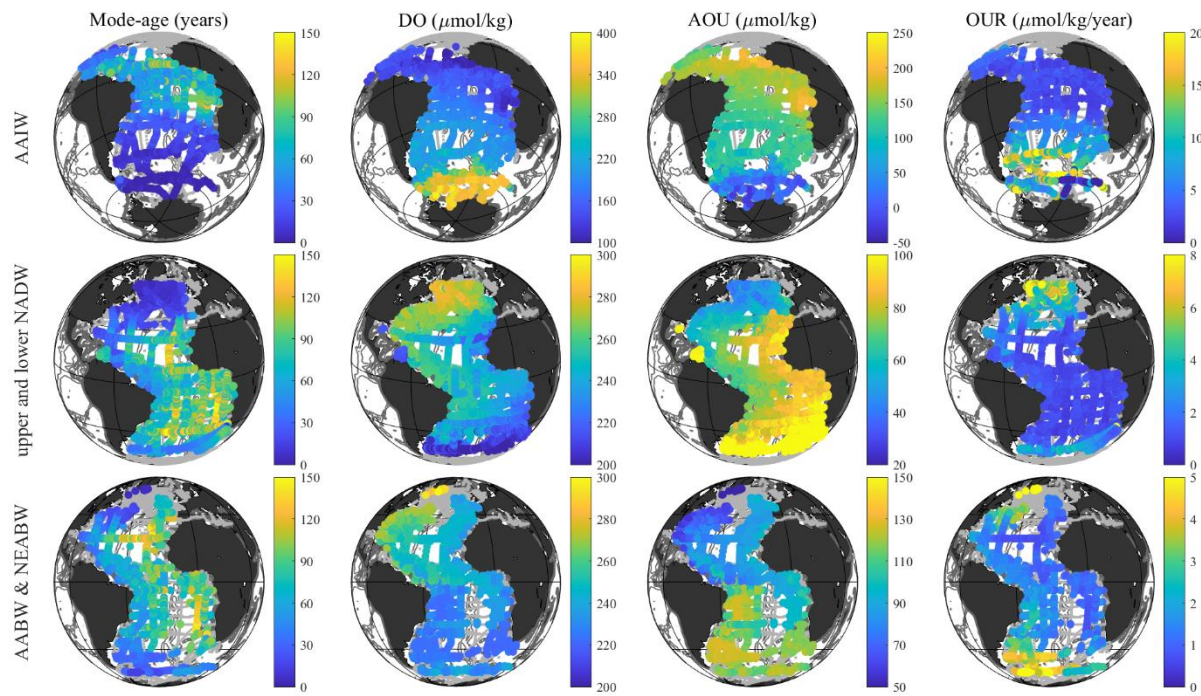


Figure 14. Mode-age, DO, AOU and OUR of wide-spread water masses in the Atlantic Ocean.

The colored dots show the values in each station at core neutral densities of each water mass (AAIW at 27.20, upper NADW at 27.95, lower NADW at 28.05, AABW at 28.15, NEABW at 28.10 kg m^{-3} , the upper and lower NADW, AABW and NEABW are shown in one plot. The grey dots show all the GLODAPv2 stations that have less than 20% contribution of the water mass in question.

385 The above four properties are also represented along the A16 section (Fig. 15). The AAIW has the lowest mode-age among the three water masses, but also the largest variations in the DO and AOU. The mode-age indicates that in total of ~40 to 60 years is needed for the main body of AAIW (fractions > 80%) to be transported to the equator (Fig 15, a). The DO decreases rapidly from 260 to below 180 $\mu\text{mol kg}^{-1}$ at the oxygen minimum zone at 20 °S, while the AOU increases from 60 to 150 $\mu\text{mol kg}^{-1}$ during the northward pathway (Fig 15, b and c). The OUR is higher than 8 $\mu\text{mol kg}^{-1} \text{ yr}^{-1}$ at the beginning and decreases to 3 $\mu\text{mol kg}^{-1} \text{ yr}^{-1}$ close to the equator (Fig 15, d). The mode-age of NADW is ~140 years at 40 °S and reaches a peak of ~160 years in the region of 20 °N due to the sluggish water exchange caused by the topography. The NADW contains the highest oxygen concentration and the lowest AOU and OUR in the abyssal Atlantic Ocean. The value of DO is 260 $\mu\text{mol kg}^{-1}$ at the starting point at 60 °N and still remains 220 $\mu\text{mol kg}^{-1}$ at 40 °S where it meets the AABW and AAIW. The AOU of NADW remains below 100 $\mu\text{mol kg}^{-1}$ during the entire pathway. The OUR of NADW is below 5 $\mu\text{mol kg}^{-1} \text{ yr}^{-1}$ close to the formation area, and below 1 $\mu\text{mol kg}^{-1} \text{ yr}^{-1}$ south of 60 °N. The transport of the main body of AABW takes in total of ~100 years from the Weddell Sea to the equator. The DO and AOU remain unchanged at 220 and 130 $\mu\text{mol kg}^{-1}$ respectively on the pathway to the equator, indicating very low OUR. Although derived from the AABW, the characteristics of the NEABW are more similar to the NADW in all the above properties.

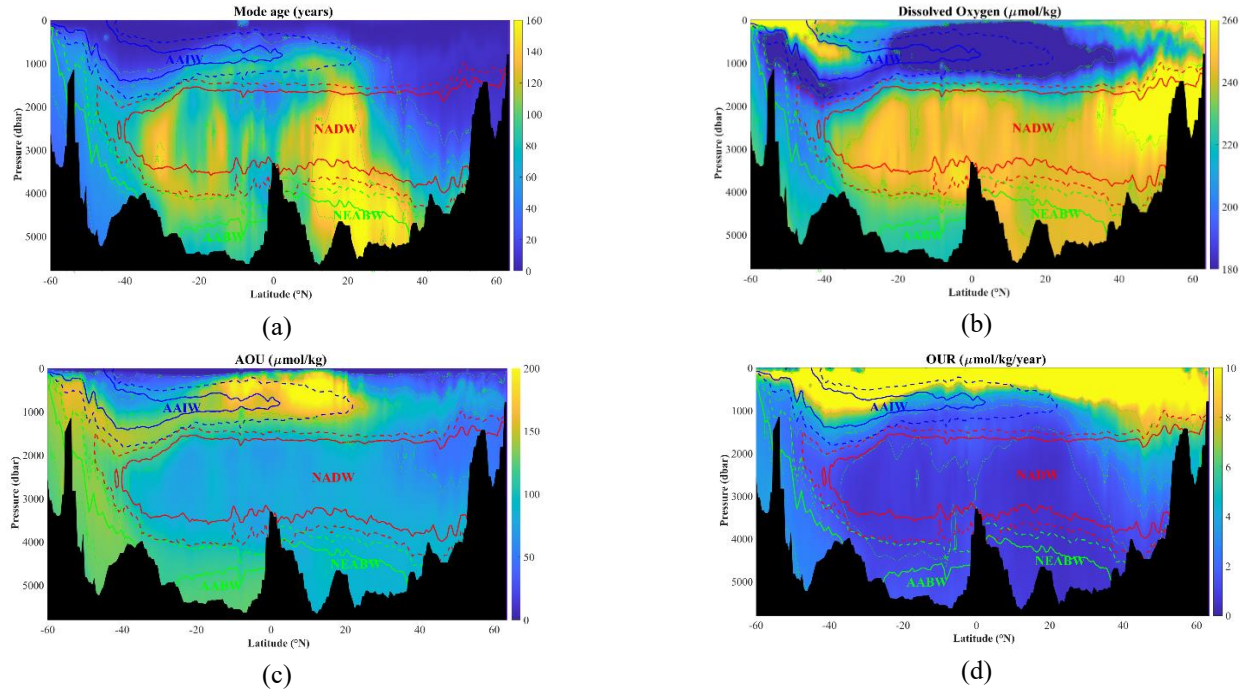


Figure 15. Distributions of mode-age (a), dissolved oxygen (b), conservative temperature (c) and AOU (d) along the A16 section line. The color solid lines show the fractions of 80% in each water mass and the dashed lines show the fractions of 50%.



400 5 Conclusions

The geographic distributions of main water masses in the Atlantic Ocean are reported in Liu and Tanhua, (2021). As the continuous work, the transports of water masses are traced by the transient tracers (CFC-12 and SF₆) and the water mass ages (consuming time during the pathway) are estimated. The assumption of a standard mixing ratio ($\Delta/\Gamma = 1$) and a saturation of 100% is followed. Three different definitions of water mass ages are investigated. The tracer-age assumes the ocean as a totally advective situation without diffusion and underestimates the actual age in the realistic ocean. The mean-age, which shows the average value of all the different parts in one water sample, is used to show the static distribution of water masses. The mode-age, which shows the age of the dominant water mass in the sample, is used to trace the biogeochemical phenomena.

In general, the water mass age increases with the pressure and distance from the formation area, so the central waters in the upper layer obtain the lowest ages of within ~100 years. In the intermediate layer, the AAIW and MW are two conspicuous water masses and both take ~300 years to spread from south to north (AAIW) and east to west (MW) respectively. As the dominant water mass in the deep and overflow layer, the NADW takes ~500 years to spread along the DWBC in the west Atlantic Ocean, and takes ~ 900 years eastward to cover the east part. The bottom waters origin from south of Antarctic Circumpolar Current region take ~600 years to spread northward and cover the bottom layer. Similar as the NADW, the mean-age of both AABW and NEABW show spatial difference between the west (low mean-age) and the east (high mean-age). This is because the west Atlantic Ocean is well ventilated by the DWBC while the water exchange is sluggish in the east.

The ventilations and respiration rates (oxidation rates) of wide-spread water masses are estimated by the mode-ages. The currents and topography have significant impacts on the mode-ages and furthermore the respiration rates. The western basins of the Atlantic Ocean are better ventilated with lower the mode-ages, while the OURs show the opposite distribution, suggesting that the mode-age is a more important determinant of OUR in seawater than AOU and higher respiration rates exist when the region is better ventilated.

420 Author contributions. ML designed the research study and conducted the analysis. ML and TT interpreted the results and wrote the paper.

Competing interests. The contact author has declared that none of the authors has any competing interests.

425 Acknowledgements

This work is based on the comprehensive and detailed data from the GLODAP data product throughout the past few decades. In particular, we are grateful to the efforts from all the scientists and crews on cruises, who generated funding and dedicated time on committing the collection of data. We also would like to thank the working groups of GLODAP for their support and information of the collation, quality control and publishing of data. Their contributions and selfless sharing are prerequisites for the completion of this work. In addition, we are grateful to Dr. Tim Stöven for his support and advices in running calculating programs of water mass ages. Thanks goes to Prof. Minggang Cai and his research group at the College of Ocean and Earth Sciences, Xiamen University for the help and support during Mian Liu's postdoctoral work, also goes to all the colleagues in School of Environmental Science and Engineering, Xiamen University of Technology.

435 Financial support. This work is supported by Natural Science Foundation of Xiamen City (3502ZZ20227214). Mian Liu received support from the China Scholarship Council (CSC) to support the PhD study at GEOMAR Helmholtz Centre for Ocean Research Kiel.



References

440 Armour, K. C., J. Marshall, J. R. Scott, A. Donohoe, and E. R. Newsom: Southern Ocean warming delayed by circumpolar upwelling and equatorward transport, *Nature Geoscience*, 9(7), 549-554, doi:10.1038/ngeo2731, 2016.

Bender, M. L.: The $\delta^{18}\text{O}$ of dissolved O_2 in seawater: A unique tracer of circulation and respiration in the deep sea, *Journal of Geophysical Research: Oceans*, 95(C12), 22243-22252, doi:<https://doi.org/10.1029/JC095iC12p22243>, 1990.

445 Bjerknes, J.: Atlantic Air-Sea Interaction, in *Advances in Geophysics*, edited by H. E. Landsberg and J. Van Mieghem, pp. 1-82, Elsevier, doi:[https://doi.org/10.1016/S0065-2687\(08\)60005-9](https://doi.org/10.1016/S0065-2687(08)60005-9), 1964.

Bryden, H. L., H. R. Longworth, and S. A. Cunningham: Slowing of the Atlantic meridional overturning circulation at 25 degrees N, *Nature*, 438(7068), 655-657, doi:10.1038/nature04385, 2005.

Bullister, J. L., and R. F. Weiss: Anthropogenic Chlorofluoromethanes in the Greenland and Norwegian Seas, *Science*, 221(4607), 265-268, doi:10.1126/science.221.4607.265, 1983.

450 Bullister, J. L., D. P. Wisegarver, and F. A. Menzia: The solubility of sulfur hexafluoride in water and seawater, *Deep Sea Research Part I: Oceanographic Research Papers*, 49(1), 175-187, doi:10.1016/s0967-0637(01)00051-6, 2002.

Clark, P. U., J. D. Shakun, P. A. Baker, P. J. Bartlein, S. Brewer, E. Brook, A. E. Carlson, H. Cheng, D. S. Kaufman, and Z. Liu: Global climate evolution during the last deglaciation, *Proceedings of the National Academy of Sciences*, 109(19), E1134-E1142, doi:10.1073/pnas.1116619109, 2012.

455 Dickson, R. R., and J. Brown: The production of North Atlantic Deep Water: Sources, rates, and pathways, *Journal of Geophysical Research: Oceans*, 99(C6), 12319-12341, doi:10.1029/94jc00530, 1994.

Doney, S. C., and J. L. Bullister: A chlorofluorocarbon section in the eastern North Atlantic, *Deep-Sea Res*, 39(11-12A), 1857-1883, doi:10.1016/0198-0149(92)90003-c, 1992.

460 Fine, R. A.: Observations of CFCs and SF_6 as Ocean Tracers, in *Annual Review of Marine Science*, Vol 3, edited by C. A. Carlson and S. J. Giovannoni, pp. 173-195, doi:10.1146/annurev.marine.010908.163933, 2011.

Gammon, R. H., J. Cline, and D. Wisegarver: Chlorofluoromethanes in the northeast Pacific Ocean: Measured vertical distributions and application as transient tracers of upper ocean mixing, *Journal of Geophysical Research-Oceans*, 87(NC12), 9441-9454, doi:10.1029/JC087iC12p09441, 1982.

Hall, M. M., and H. L. Bryden: Direct Estimates and Mechanisms of Ocean Heat-Transport, *Deep-Sea Res*, 29(3), 339-359, doi:10.1016/0198-0149(82)90099-1, 1982.

Hall, T. M., and R. A. Plumb: Age as a diagnostic of stratospheric transport, *Journal of Geophysical Research-Atmospheres*, 99(D1), 1059-1070, doi:10.1029/93jd03192, 1994.



Huhn, O., M. Rhein, M. Hoppema, and S. van Heuven: Decline of deep and bottom water ventilation and slowing down of anthropogenic carbon storage in the Weddell Sea, 1984-2011, Deep Sea Research Part I: Oceanographic Research Papers, 76, 470 66-84, doi:10.1016/j.dsr.2013.01.005, 2013.

Ito, T., A. Nenes, M. S. Johnson, N. Meskhidze, and C. Deutsch: Acceleration of oxygen decline in the tropical Pacific over the past decades by aerosol pollutants, *Nature Geoscience*, 9(6), 443-447, doi:10.1038/ngeo2717, 2016.

Jenkins, W. J.: Oxygen utilization rates in North Atlantic subtropical gyre and primary production in oligotrophic systems, *Nature*, 300(5889), 246-248, doi:10.1038/300246a0, 1982.

475 Jenkins, W. J.: ^3H and ^3He in the Beta Triangle: Observations of Gyre Ventilation and Oxygen Utilization Rates, *Journal of Physical Oceanography*, 17(6), 763-783, doi:10.1175/1520-0485(1987)017<0763:Aitbto>2.0.Co;2, 1987.

Karstensen, J., and M. Tomczak, Ventilation processes and water mass ages in the thermocline of the southeast Indian Ocean, *Geophysical Research Letters*, 24(22), 2777-2780, doi:10.1029/97gl02708, 1997.

480 Karstensen, J., and M. Tomczak: Age determination of mixed water masses using CFC and oxygen data, *Journal of Geophysical Research-Oceans*, 103(C9), 18599-18609, doi:10.1029/98jc00889, 1998.

Karstensen, J., L. Stramma, and M. Visbeck: Oxygen minimum zones in the eastern tropical Atlantic and Pacific oceans, *Progress in Oceanography*, 77(4), 331-350, doi: 10.1016/j.pocean.2007.05.009, 2008.

Kirchner, K., M. Rhein, S. Huttli-Kabus, and C. W. Böning: On the spreading of South Atlantic Water into the Northern Hemisphere, *Journal of Geophysical Research-Oceans*, 114, doi:10.1029/2008jc005165, 2009.

485 Koeve, W., and P. Kähler: Oxygen utilization rate (OUR) underestimates ocean respiration: A model study, *Global Biogeochemical Cycles*, 30(8), 1166-1182, doi:10.1002/2015gb005354, 2016.

Kuhlbrodt, T., A. Griesel, M. Montoya, A. Levermann, M. Hofmann, and S. Rahmstorf: On the driving processes of the Atlantic meridional overturning circulation, *Reviews of Geophysics*, 45(1), doi:10.1029/2004rg000166, 2007.

490 Liu, M., and T. Tanhua: Water masses in the Atlantic Ocean: characteristics and distributions, *Ocean Science*, 17(2), 463-486, doi:10.5194/os-17-463-2021, 2021.

Maiss, M., L. P. Steele, R. J. Francey, P. J. Fraser, R. L. Langenfelds, N. B. A. Trivett, and I. Levin: Sulfur hexafluoride - A powerful new atmospheric tracer, *Atmospheric Environment*, 30(10-11), 1621-1629, doi:10.1016/1352-2310(95)00425-4, 1996.

495 Morrison, A. K., T. L. Frölicher, and J. L. Sarmiento: Upwelling in the Southern Ocean, *Physics Today*, 68(1), 27-32, doi:10.1063/pt.3.2654, 2015.

Orsi, A. H., G. C. Johnson, and J. L. Bullister: Circulation, mixing, and production of Antarctic Bottom Water, *Progress in Oceanography*, 43(1), 55-109, doi:10.1016/s0079-6611(99)00004-X, 1999.

Patara, L., C. W. Böning, and T. Tanhua: Multidecadal Changes in Southern Ocean Ventilation since the 1960s Driven by Wind



and Buoyancy Forcing, *Journal of Climate*, 34(4), 1485-1502, doi:10.1175/Jcli-D-19-0947.1, 2021.

500 Purkey, S. G., and G. C. Johnson: Warming of Global Abyssal and Deep Southern Ocean Waters between the 1990s and 2000s: Contributions to Global Heat and Sea Level Rise Budgets, *Journal of Climate*, 23(23), 6336-6351, doi:10.1175/2010jcli3682.1, 2010.

Pytkowicz, R. M.: On the apparent oxygen utilization and the preformed phosphate in the oceans1, *Limnology and Oceanography*, 16(1), 39-42, <https://doi.org/10.4319/lo.1971.16.1.0039>, 1971.

505 Rahmstorf, S.: The Great Ocean Conveyor: Discovering the Trigger for Abrupt Climate Change, *Nature*, 464(7289), 681-681, doi:10.1038/464681a, 2010.

Redfield, A. C.: The processes determining the concentration of oxygen, phosphate and other organic derivatives within the depths of the Atlantic Ocean, *Pap. Phys. Oceanogr. Meteorol. Mass. Inst. Technol. Woods Hole Oceanogr. Inst.*, 9, 1-22, <https://doi.org/10.1575/1912/1053>, 1942.

510 Redfield, A. C., B. H. Ketchum, F. A. Richards, The influence of organisms on the composition of seawater, *The Sea. Ideas and Observations on Progress in the Study of the Seas* M. N. Hill, 26-77, John Wiley, New York, 1963.

Sandström, J. W.: Dynamishce versuche mit merrwasser. *Annalen der Hydrographie und Maritimen Meteorologie*, 36, 6-23, 1908.

515 Sandström, J. W.: Meteorologische studien im Schwedischen Hochgebirge. *Göteborgs Kungl. Vetenskaps- och Vitterhetssamhälles Handlingar*, 17, 1-48, 1916.

Schmidtko, S., L. Stramma, and M. Visbeck: Decline in global oceanic oxygen content during the past five decades, *Nature*, 542(7641), 335-339, doi:10.1038/nature21399, 2017.

Schneider, A., T. Tanhua, A. Kortzinger, and D. W. R. Wallace: High anthropogenic carbon content in the eastern Mediterranean, *Journal of Geophysical Research-Oceans*, 115, doi:10.1029/2010jc006171, 2010.

520 Skinner, L. C., F. Primeau, E. Freeman, M. de la Fuente, P. A. Goodwin, J. Gottschalk, E. Huang, I. N. McCave, T. L. Noble, and A. E. Scrivner: Radiocarbon constraints on the glacial ocean circulation and its impact on atmospheric CO₂, *Nature Communications*, 8, doi:10.1038/ncomms16010, 2017.

Sonnerup, R. E., S. Mecking, and J. L. Bullister: Transit time distributions and oxygen utilization rates in the Northeast Pacific Ocean from chlorofluorocarbons and sulfur hexafluoride, *Deep-Sea Res Pt I*, 72, 61-71, doi:10.1016/j.dsr.2012.10.013, 2013.

525 Sonnerup, R. E., S. Mecking, J. L. Bullister, and M. J. Warner: Transit time distributions and oxygen utilization rates from chlorofluorocarbons and sulfur hexafluoride in the Southeast Pacific Ocean, *Journal of Geophysical Research-Oceans*, 120(5), 3761-3776, doi:10.1002/2015jc010781, 2015.

Stanley, R. H. R., S. C. Doney, W. J. Jenkins, and D. E. Lott: Apparent oxygen utilization rates calculated from tritium and helium-3 profiles at the Bermuda Atlantic Time-series Study site, *Biogeosciences*, 9(6), 1969-1983, doi:10.5194/bg-9-1969-2012, 2012.



Stöven, T., and T. Tanhua: Ventilation of the Mediterranean Sea constrained by multiple transient tracer measurements, *Ocean Science*, 10(3), 439-457, doi:10.5194/os-10-439-2014, 2014.

Sverdrup, H. U.: The unity of the sciences of the sea, *Sigma Xi Quarterly*, 28(3), 105-115, <https://www.jstor.org/stable/23049117>, 1940.

535 Talley, L.: Antarctic Intermediate Water in the South Atlantic, in *The South Atlantic: Present and Past Circulation*, edited by G. Wefer, W. H. Berger, G. Siedler and D. J. Webb, pp. 219-238, Springer Berlin Heidelberg, Berlin, Heidelberg, doi:10.1007/978-3-642-80353-6_11, 1996.

Talley, L.: Closure of the Global Overturning Circulation Through the Indian, Pacific, and Southern Oceans: Schematics and Transports, *Oceanography*, 26(1), 80-97, doi:10.5670/oceanog.2013.07, 2013.

540 Talley, L., R. Feely, B. Sloyan, R. Wanninkhof, M. Baringer, J. Bullister, C. Carlson, S. Doney, R. Fine, and E. Firing, N. Gruber, D.A. Hansell, M. Ishii, G.C. Johnson, K. Katsumata, R.M. Key, M. Kramp, C. Langdon, A.M. Macdonald, J.T. Mathis, E.L. McDonagh, S. Mecking, F.J. Millero, C.W. Mordy, T. Nakano, C.L. Sabine, W.M. Smethie, J.H. Swift, T. Tanhua, A.M. Thurnherr, M.J. Warner, and J.-Z. Zhang: Changes in ocean heat, carbon content, and ventilation: A review of the first decade of GO-SHIP global repeat hydrography, *Annual review of marine science*, 8, 185-215, <https://doi.org/10.1146/annurev-marine-052915-100829>, 2016.

545

Tamsitt, V., H. F. Drake, A. K. Morrison, L. D. Talley, C. O. Dufour, A. R. Gray, S. M. Griffies, M. R. Mazloff, J. L. Sarmiento, J. Wang, W. Weijer: Spiraling pathways of global deep waters to the surface of the Southern Ocean, *Nature Communications*, 8(1), 172, doi:10.1038/s41467-017-00197-0, 2017.

550

Tanhua, T., A. Biastoch, A. Kortzinger, H. Luger, C. Boning, and D. W. R. Wallace: Changes of anthropogenic CO₂ and CFCs in the North Atlantic between 1981 and 2004, *Global Biogeochemical Cycles*, 20(4), doi:10.1029/2006gb002695, 2006.

Tanhua, T., D. W. Waugh, and D. W. R. Wallace: Use of SF₆ to estimate anthropogenic CO₂ in the upper ocean, *Journal of Geophysical Research-Oceans*, 113(C4), doi:10.1029/2007jc004416, 2008.

Tanhua, T., D. W. Waugh, and J. L. Bullister: Estimating changes in ocean ventilation from early 1990s CFC-12 and late 2000s SF₆ measurements, *Geophysical Research Letters*, 40(5), 927-932, doi:10.1002/grl.50251, 2013.

555

Tanhua, T., and M. Liu: Upwelling velocity and ventilation in the Mauritanian upwelling system estimated by CFC-12 and SF₆ observations, *Journal of Marine Systems*, 151, 57-70, doi:10.1016/j.jmarsys.2015.07.002, 2015.

Thiele, G., and J. L. Sarmiento: Tracer Dating and Ocean Ventilation, *Journal of Geophysical Research-Oceans*, 95(C6), 9377-9391, doi:10.1029/JC095iC06p09377, 1990.

560

Thomas, J. L., D. W. Waugh, and A. Gnanadesikan: Relationship between Age and Oxygen along Line W in the Northwest Atlantic Ocean, *Ocean Science Journal*, 55(2), 203-217, doi:10.1007/s12601-020-0019-5, 2020.

Tomczak, M.: Some historical, theoretical and applied aspects of quantitative water mass analysis, *Journal of Marine Research*, 57(2), 275-303, doi:10.1357/002224099321618227, 1999.



Tseitlin, V.: Depth dependence of oxygen utilization rate, OKEANOLOGIYA, 32(2), 264-269, 1992.

565 van Heuven, S., M. Hoppema, O. Huhn, H. A. Slagter, and H. J. W. de Baar: Direct observation of increasing CO₂ in the Weddell Gyre along the Prime Meridian during 1973-2008, Deep-Sea Research Part II-Topical Studies in Oceanography, 58(25-26), 2613-2635, doi:10.1016/j.dsr2.2011.08.007, 2011.

Wang, W. M., M. G. Cai, P. Huang, H. W. Ke, M. Liu, L. H. Liu, H. X. Deng, B. J. Luo, C. H. Wang, X. H. Zheng, W. Q. Li: Transit Time Distributions and Apparent Oxygen Utilization Rates in Northern South China Sea Using Chlorofluorocarbons and Sulfur Hexafluoride Data, Journal of Geophysical Research-Oceans, 126(8), doi:10.1029/2021jc017535, 2021.

570 Warner, M. J., and R. F. Weiss: Solubility of Chlorofluorocarbon-11 and Chlorofluorocarbon-12 in water and seawater, Deep-Sea Res, 32(12), 1485-1497, doi:10.1016/0198-0149(85)90099-8, 1985.

Waugh, D. W., T. M. Hall, and T. W. N. Haine: Relationships among tracer ages, Journal of Geophysical Research: Oceans, 108(C5), doi:10.1029/2002jc001325, 2003.

575 Waugh, D. W., T. W. N. Haine, and T. M. Hall: Transport times and anthropogenic carbon in the subpolar North Atlantic Ocean, Deep Sea Research Part I: Oceanographic Research Papers, 51(11), 1475-1491, doi:10.1016/s0967-0637(04)00145-1, 2004.

Ziska, F., B. Quack, K. Abrahamsson, S. D. Archer, E. Atlas, T. Bell, J. H. Butler, L. J. Carpenter, C. E. Jones, N. R. P. Harris, H. Hepach, K. G. Heumann, C. Hughes, J. Kuss, K. Krüger, P. Liss, R. M. Moore, A. Orlikowska, S. Raimund, C. E. Reeves, W. Reifenhäuser, A. D. Robinson, C. Schall, T. Tanhua, S. Tegtmeier, S. Turner, L. Wang, D. Wallace, J. Williams, H. Yamamoto, S. Yvon-Lewis, and Y. Yokouchi: Global sea-to-air flux climatology for bromoform, dibromomethane and methyl iodide, Atmospheric Chemistry and Physics, 13(17), 8915-8934, doi:10.5194/acp-13-8915-2013, 2013.